

A high resolution hindcast of the meteorological sea level component for Southern Europe: the GOS dataset

Alba Cid · Sonia Castanedo · Ana J. Abascal ·
Melisa Menéndez · Raúl Medina

Received: 16 September 2013 / Accepted: 24 December 2013 / Published online: 12 January 2014
© Springer-Verlag Berlin Heidelberg 2014

Abstract Two sets of 62-year (1948–2009) and 21-year (1989–2009) high-resolution hindcasts of the meteorological sea level component have been developed for Southern Europe using the Regional Ocean Model System (ROMS) of Rutgers University. These new databases, named *GOS 1.1* and *GOS 2.1*, are a valuable tool for a wide variety of studies, such as those related to a better understanding of sea level variability, flooding risk and coastal engineering studies. The model domain encloses Southern Europe, including the Mediterranean Sea and the Atlantic coast, with a horizontal resolution of $1/8^\circ$ (~ 14 km). In order to study the effect of the atmospheric forcing resolution, ROMS is driven with two different regional atmospheric forcings: SeaWind I (30 km of horizontal resolution) and SeaWind II (15 km of horizontal resolution). Both are the result of a dynamical downscaling from global atmospheric reanalysis: NCEP global reanalysis and ERA-Interim global reanalysis, respectively. As a result, two surge data sets are obtained: GOS 1.1 (forced with SeaWind I) and GOS 2.1 (forced with SeaWind II). Surge elevations calculated by ROMS are compared with in situ measurements from tide gauges in coastal areas and with open ocean satellite observations. The validation procedure, testing outcomes from GOS 1.1 and GOS 2.1 against observations, shows the capability of the model to simulate accurately the sea level variation induced by the meteorological forcing. A description of the surge in terms of seasonality and long term trends is also made. The climate variability analysis

reveals clear seasonal patterns in the Mediterranean Sea basins. A long-term negative trend for the period 1948–2009 is found, whilst positive trends are computed for the last 20 years (GOS 2.1).

Keywords ROMS · Non-tidal residuals · Storm surge · Trends · Numerical modelling · Satellite validation

1 Introduction

There is an increasing interest in studying the sea surface response to the atmospheric pressure and wind forcing due to its important contribution to sea level during flood events. Coastal areas are particularly vulnerable to climate variability and change. Storm surges, which are primarily caused by low pressure and strong winds, are affected by changes in climate patterns (Flather et al. 1998; Lowe et al. 2001; Woth et al. 2005). As a consequence, coastal flooding and management practices could also be affected. In order to understand these changes, long time series describing these phenomena are required. Unfortunately, real data provided by measurement networks are scarce and presents severe limitations, both in terms of spatial and temporal coverage. Moreover, observations usually contain gaps and irregular sampling, which introduces difficulties and uncertainties into the study. In order to overcome these limitations, numerical models have become one of the most useful tools for generating long-term and high resolution (in time and space) databases. Numerical models have the advantage of being able to generate long-time series of atmospheric and ocean variables for periods when no observation is available. This makes surge hindcasts a relevant tool in many scientific and engineering studies.

A. Cid (✉) · S. Castanedo · A. J. Abascal · M. Menéndez ·
R. Medina
Environmental Hydraulics Institute “IH Cantabria”,
Universidad de Cantabria, C/Isabel Torres No. 5, PCTCAN,
39011 Santander, Spain
e-mail: alba.cid@unican.es

In recent years, many studies have aimed at understanding and quantifying changes in storm surge by means of numerically generated databases. These databases can be analysed in the same way as observations for a wide variety of studies addressing extreme values (Flather et al. 1998; Marcos et al. 2009), decadal variations (Butler et al. 2007), frequency of storm surges (Bernier and Thompson 2006) or climate change effects on storm surge (Flather and Williams 2000; Wang et al. 2008; Jordà et al. 2012).

With respect to Southern Europe, Sebastião et al. (2008) has performed a sea level hindcast for the Atlantic coast of Europe (including astronomic and meteorological effects). There is also the hindcast presented by Ratsimandresy et al. (2008) for the Mediterranean Sea. Both hindcasts were performed for the period 1958–2001 using a barotropic model (HAMSOM model (Backhaus 1985)) with a grid size of 10' in longitude and 15' in latitude. In both cases, the model was driven with wind and pressure fields with a resolution of $0.5^\circ \times 0.5^\circ$. These atmospheric fields were created by means of dynamical downscaling from the global reanalysis NCEP, using the limited area model (LAM) REMO (Jacob and Podzun 1997). There is also a new study on storm surge for the Mediterranean Sea, with focus on the Italian coast, where a model coupling waves, astronomical tide and storm surge has been developed (Ferrarin et al. 2013). In this work, the atmospheric data fields are produced by a meteorological model chain, from global to local scale.

Nowadays, in order to reproduce mesoscale phenomena, efforts are directed towards increasing the resolution of the atmospheric forcing fields in storm surge numerical simulations (Jones and Davies 2006; Wang et al. 2008; Brown et al. 2010). Thus, high resolution atmospheric fields are required for simulating more accurately this sea level component. In this work, two different atmospheric forcings have been used in order to investigate the sensitivity of the results to the resolution of the atmospheric fields. This resulted in the generation of two high resolution surge hindcast for Southern Europe. The obtained regional data sets belong to the GOS (Global Ocean Surges) database (the American GOS dataset is described in Losada et al. 2013). These data sets represent the sea level variation due to wind and pressure for continuous series of meteorological fields, not only specific simulations during storms. Therefore, hereafter we will use the term storm surge when referring to the wind and atmospheric pressure contribution to the total sea level.

It is important to highlight that these hindcasts enclose the whole Southern European coast, including the Canary Islands region (see Fig. 1). Up to now, none of the existing databases provide information that westward. This reveals the importance of the present work and its applicability to

current studies in the area (for instance, coastal dynamic studies related to desalinization plants).

The European GOS data sets have been performed using the Regional Ocean Model System (ROMS) (Shchepetkin and McWilliams 2005), and using two different atmospheric forcings: SeaWind I (30 km of horizontal resolution) and SeaWind II (15 km of horizontal resolution). These atmospheric fields have been obtained by a dynamical downscaling from NCEP and ERA-Interim global reanalysis, respectively, and they have been exhaustively validated with observations (more details in Menéndez et al. 2013). The influence of the forcing resolution into the storm surge elevation is analysed by means of the comparison of both datasets with observed data.

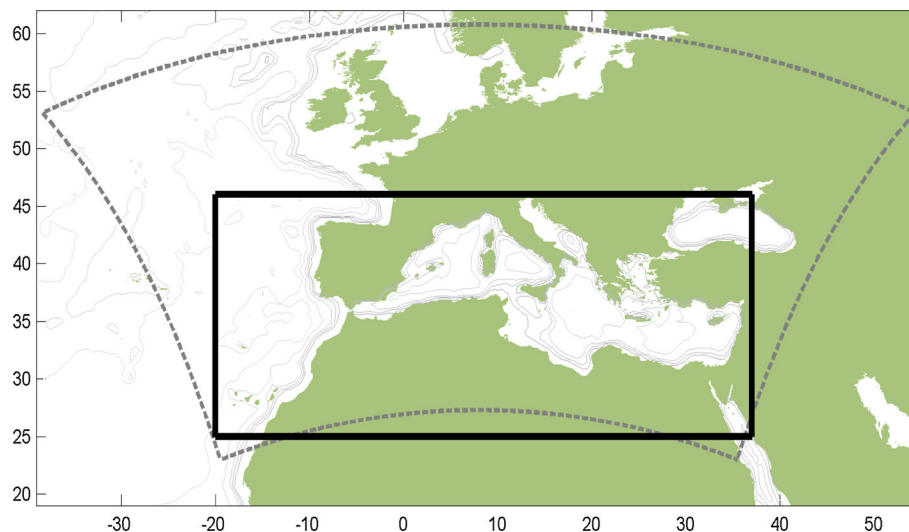
Special attention is focused on the validation of the storm surge numerical results. Surge elevations calculated by ROMS model in the two runs are exhaustively compared with values measured by 58 tide gauges distributed across the domain. In areas where no observations are available, validation is made by the use of altimetry data. As far as the authors' knowledge, validation of storm surge with satellite data has been previously done by Wang et al. (2008), only for Irish waters. Thus, this is the first attempt in validating the results from a storm surge numerical model using altimetry data in a large area, covering all Southern Europe. Satellite altimeter data were also used by Calafat and Gomis (2009) to reconstruct and validate sea level fields in the Mediterranean Sea. In this work a comparison between the model results and altimetry data is made all over the domain. The satellite validation is a step forward with respect to previous works, where validations were performed only with tide gauges, covering few locations of the whole domain.

The aim of this paper is not only the presentation of the two storm surge databases but also the analysis of the seasonal variability and long term trends using GOS hindcasts. Results show clear seasonal patterns as well as different trends when averaging different periods, as already suggested by Gomis et al. (2008).

The main objectives of this work are: (1) The description of the two data sets, (2) its validation with tide gauges and satellite data, (3) obtaining the influence of the forcing resolution on the storm surge results by comparing the two datasets and (4) the application of GOS database to study variability and trends.

The organization of this paper is as follows: The model description and configuration is described in Sect. 2. Section 3 is devoted to verify the modelling results by comparing them with satellite and tide gauge data. Seasonal patterns and estimated long-term trends of the meteorological sea level component are analyzed in Sect. 4. Finally, the main conclusions are summarized in Sect. 5.

Fig. 1 Grid domain of storm surge hindcast (*black line*) and atmospheric downscaling (*dashed gray line*)



2 Model set-up

Storm surge has been simulated using the Regional Ocean Model System (ROMS) developed by Rutgers University. ROMS is a three-dimensional, free-surface, terrain-following ocean model that solves the Reynolds-averaged Navier–Stokes equations using the hydrostatic vertical momentum balance and Boussinesq approximation with a split-explicit time stepping algorithm (Haidvogel et al. 2000; Shchepetkin and McWilliams 2005; Haidvogel et al. 2008). It uses a horizontal curvilinear Arakawa C grid and vertical stretched terrain-following coordinates.

The model is set-up for Southern Europe covering the area shown in Fig. 1, which spans from 25° to 46°N in latitude and from 20°W to 37°E in longitude with a horizontal resolution of 1/8°. The bathymetry is extracted from the ETOPO 2 database, a global topography of 2 min resolution derived from depth soundings and satellite gravity observations (Smith and Sandwell 1997).

In this study, ROMS model is run in barotropic mode. The inverted barometer effect is imposed at the open boundaries of the domain (North and West), using a free surface Chapman condition and 2D Flather condition for momentum. Note that non-linear energy transfer between tides and surges is very low off the Spanish coast (Carretero et al. 2000; Ratsimandresy et al. 2008), and the microtidal environment of the Mediterranean Sea reduces the nonlinear interaction between tides and storm surges (Lionello 2012). Based on these features of the study area at this scale and resolution, it is possible to perform and independent model computation of residuals, without taking into account the nonlinear transfer of tidal energy. Bottom stress is given by a quadratic bottom drag coefficient of 10^{-4} . Horizontal viscosity is set using a lateral, harmonic, constant mixing coefficient of $500 \text{ m}^2/\text{s}$. The

model is driven with hourly meteorological data of wind and atmospheric pressure provided by dynamical downscalings developed within the framework of the SeaWind project (more details in Menéndez et al. (2013)). The atmospheric downscaling was performed using the Research and Forecasting model with the Advanced Research dynamical solver (WRF–ARW) (Skamarock et al. 2008). SeaWind grid domain covers the European region and the whole Mediterranean Sea (see Fig. 1). SeaWind dataset consist of two different atmospheric hindcasts: SeaWind I (30 km horizontal resolution for a period of 62 years) and SeaWind II (15 km horizontal resolution for a 21-year period). SeaWind I is based on the NCEP global reanalysis I (Kalnay et al. 1996) and SeaWind II is based on the ERA-Interim global reanalysis (Dee et al. 2011). Both downscalings were interpolated to the ROMS grid at 1/8° horizontal resolution.

As a summary, two storm surge hindcasts are performed: (1) GOS 1.1 which is an hourly dataset of 1/8° spatial resolution for the 1948–2009 period forced with SeaWind I; and (2) GOS 2.1 consisting of an hourly dataset of 1/8° spatial resolution for the 1989–2009 period forced with SeaWind II.

3 Hindcast validation

3.1 Tide gauges versus modelled data

Model results are validated using in situ measurements from local tide gauges. This work makes use of tide gauge records from different sources: Puertos del Estado (PdE) (www.puertos.es), University of Hawaii Sea Level Center (UHSLC) (<http://uhslc.soest.hawaii.edu>), Système d’Observation du Niveau des Eaux Littorales (SONEL)

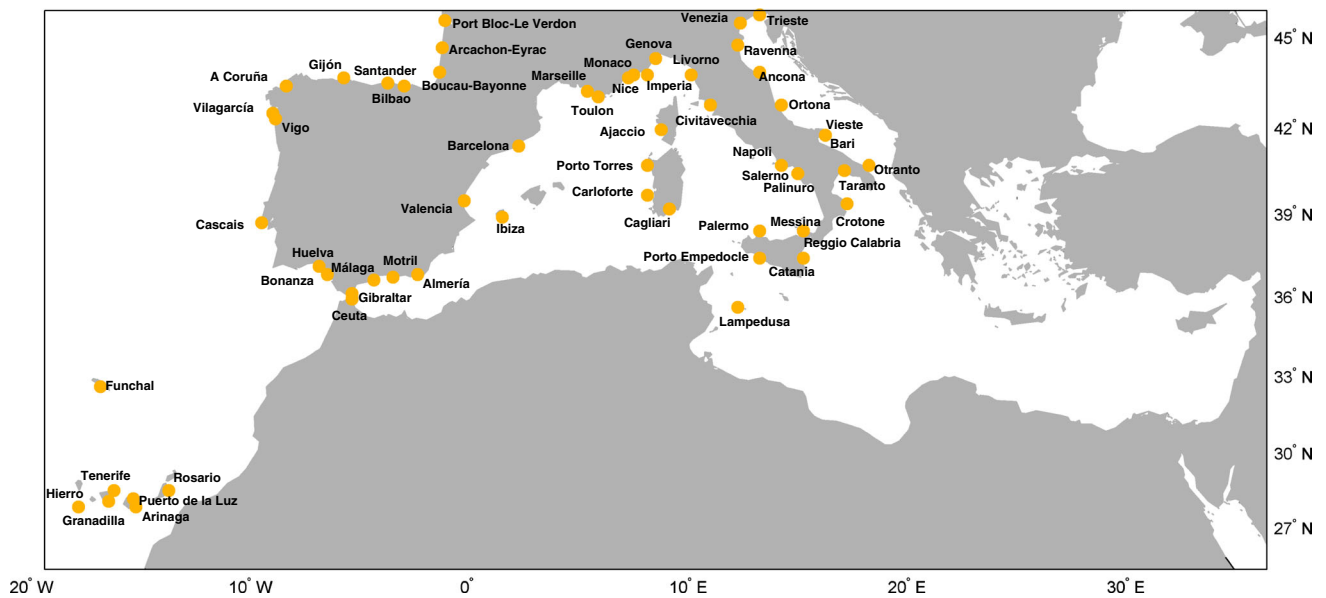


Fig. 2 Location of the tide gauges used to validate the storm surge hindcasts

(<http://www.sonel.org>) and Istituto Superiore per la Protezione e la Ricerca Ambientale (ISPRA) (www.idromare.it). Figure 2 illustrates the location of the tide gauge stations used in the validation, which cover a wide area within the computational domain, both in Atlantic and Mediterranean coast. Although there are several tide gauges along the east Adriatic and few more stations along the Turkey coast, they have not been considered because their length and quality are not adequate for a representative validation of the model results. A summary of the tide gauges data is presented in Table 1, including the name of the station, owner institution and available data periods. Observations as well as numerical simulations provide hourly data. Modelled time series are extracted at these locations (closest GOS grid point to the tide gauge) and compared with the observed residual (observed total elevation minus predicted tide) from the in situ measurements. Predicted tide at each tide gauge station is calculated using t-tide package (Pawlowicz et al. 2002). Each year is analysed separately, and in the case of too many gaps in the tide gauge time series for a specific year, the tidal analysis for that period is not performed. Tidal constituents included in the analysis are those with a noise-signal ratio >2 , except for the annual and semi-annual components that have not been removed because, as previous authors indicate (Pascual et al. 2008), the main contributors to this particular signals are thermosteric and meteorological rather than astronomical. The mean sea level of the entire time series at each station is subtracted from the non-tidal residuals to obtain storm surge anomalies. Mean level at each grid point of the numerical data is subtracted from the modelled series in order to also have “anomalies” in the hindcast

results. Throughout the rest of this paper when speaking about non-tidal residuals from tide gauges or simulated storm surge, we refer to anomalies.

Figure 3 shows the time series comparison for 3 stations in the Atlantic area (Santander, Huelva and Arinaga; a, b and c, respectively) and 3 stations in the Mediterranean basin (Genova, Porto Torres and Palermo; d, e and f, respectively). A period of 3 months (Jan–Mar) for the year 2004 is presented. The grey line represents the non-tidal residuals extracted from the tide gauges, while red and blue lines correspond to the storm surge hindcast (GOS 1.1 and GOS 2.1 respectively). The hourly time series comparison shows a good agreement, both in terms of magnitude and timing of the surge events. As can be seen, results from GOS 1.1 and GOS 2.1 are very similar.

In order to quantify the accuracy of the simulations, a statistical analysis is carried out. Key statistical parameters such as correlation factors and root mean square errors (RMSE) are calculated at each location. As an example, Fig. 4 depicts the diagnostic plots for GOS 2.1 at the same stations mentioned in Fig. 3. The panels show the scatter, quantile–quantile plot, and statistical indices of observed versus modelled data. Colours indicate the sample density (red for high density and blue for low data density). The solid line corresponds to $y = x$ (modelled equal to observed data). 30 quantiles are estimated on a equally spaced Gumbel probability distribution, which allows a more detailed representation of the higher values. Solid circles show quantiles above the 90th percentile. The number of data in the dataset (NObs), RMSE and the correlation coefficient (ρ) are also shown. Correlation coefficients are significant at 95 % confidence interval. It

Table 1 Statistical parameters of comparison between observed and hindcasts (GOS 1.1 and GOS 2.1)

Tide-gauge station	Data provider	Initial date	Final date	GOS 1.1 dataset		GOS 2.1 dataset	
				ρ	RMSE (cm)	ρ	RMSE (cm)
A Coruña	PdE	1992	2008	0.87	6.60	0.88	6.47
Ajaccio	SONEL	1981	2003	0.79	7.62	0.80	7.31
Almería	PdE	2006	2009	0.73	8.20	0.74	8.01
Ancona	ISPRA	1986	2011	0.66	15.07	0.68	14.35
Arcachon-Eyrac	SONEL	1967	2004	0.81	10.05	0.81	9.61
Arinaga	PdE	2003	2009	0.79	4.48	0.79	4.42
Barcelona	PdE	1992	2008	0.80	7.98	0.80	7.82
Bari	ISPRA	1979	2011	0.64	12.48	0.74	9.11
Bilbao	PdE	1992	2009	0.86	6.48	0.86	6.42
Bonanza	PdE	1992	2009	0.81	7.76	0.82	7.48
Boucau-Bayonne	SONEL	1967	2004	0.83	9.51	0.83	9.50
Cagliari	ISPRA	1986	2011	0.75	8.57	0.75	8.46
Carloforte	ISPRA	1988	2011	0.77	7.65	0.77	7.60
Cascais	UHSLC	1971	1999	0.82	6.55	0.82	6.99
Catania	ISPRA	1970	2011	0.79	7.17	0.79	7.18
Ceuta	UHSLC	1970	2006	0.72	8.11	0.79	6.30
Civitavecchia	ISPRA	1973	2012	0.75	8.16	0.77	7.67
Crotone	ISPRA	1991	2011	0.76	10.33	0.76	10.12
Funchal	UHSLC	1977	2005	0.79	6.51	0.80	6.46
Genova	ISPRA	1998	2011	0.78	7.66	0.80	7.28
Gibraltar	UHSLC	1970	1997	0.69	9.14	0.75	8.62
Gijón	PdE	1995	2009	0.88	6.38	0.88	6.32
Granadilla	PdE	2003	2009	0.77	5.69	0.77	5.64
Hierro	PdE	2003	2009	0.77	5.75	0.78	5.69
Huelva	PdE	1996	2009	0.81	7.51	0.82	7.16
Ibiza	PdE	2003	2009	0.78	7.75	0.78	7.57
Imperia	ISPRA	1986	2011	0.79	7.02	0.80	6.85
Lampedusa	ISPRA	1998	2011	0.73	8.95	0.73	8.79
Livorno	ISPRA	1972	2011	0.78	8.12	0.80	7.64
Málaga	PdE	1992	2009	0.72	8.61	0.74	7.92
Marseille	SONEL	1985	2004	0.81	7.30	0.82	7.42
Messina	ISPRA	1973	2012	0.79	6.79	0.79	6.72
Monaco	SONEL	1960	2004	0.76	7.27	0.79	6.88
Motril	PdE	2004	2008	0.72	8.83	0.73	8.41
Napoli	ISPRA	1986	2011	0.79	6.52	0.80	6.34
Nice	SONEL	1981	2004	0.79	7.10	0.80	6.90
Ortona	ISPRA	1986	2011	0.69	11.94	0.71	11.34
Otranto	ISPRA	1987	2011	0.72	9.05	0.74	8.71
Palermo	ISPRA	1992	2011	0.80	6.02	0.81	5.93
Palinuro	ISPRA	1987	2011	0.78	6.91	0.79	6.74
Port Bloc-Le Verdon	SONEL	1959	2004	0.82	11.24	0.83	10.15
Porto Empedocle	ISPRA	1973	2011	0.74	7.85	0.75	7.65
Porto Torres	ISPRA	1985	2011	0.77	7.34	0.78	7.24
Puerto de la Luz	UHSLC	1975	2006	0.80	4.73	0.80	4.59
Ravenna	ISPRA	1975	2011	0.59	18.72	0.62	17.35
Reggio Calabria	ISPRA	1998	2012	0.78	7.17	0.78	7.18
Rosario	PdE	2003	2009	0.78	5.00	0.78	4.92

Table 1 continued

Tide-gauge station	Data provider	Initial date	Final date	GOS 1.1 dataset		GOS 2.1 dataset	
				ρ	RMSE (cm)	ρ	RMSE (cm)
Salerno	ISPRA	1991	2011	0.75	9.07	0.75	8.90
Santander	PdE	1992	2009	0.86	6.81	0.86	6.74
Taranto	ISPRA	1991	2011	0.74	8.83	0.76	8.22
Tenerife	PdE	1992	2009	0.78	6.59	0.78	6.49
Toulon	SONEL	1961	2004	0.81	7.25	0.83	6.46
Trieste	ISPRA	1988	2011	0.61	19.55	0.64	18.07
Valencia	PdE	1992	2006	0.75	9.46	0.77	8.93
Venezia	ISPRA	1986	2011	0.61	20.20	0.64	18.46
Vieste	ISPRA	1990	2011	0.75	9.38	0.77	8.88
Vigo	PdE	1992	2009	0.88	6.53	0.89	6.34
Vilagarcía	PdE	1997	2009	0.86	7.80	0.87	7.68

The root mean square error (RMSE) and the correlation index (ρ) are displayed

can be observed the good agreement reached between measured and hindcasted values. High correlations values (0.78–0.86) and small RMSE (4.42–7.28 cm) are obtained both in Atlantic and Mediterranean coast. The majority of data (red areas in Fig. 4) are around the bisector, although slight discrepancies can be seen at the upper tail of the quantiles. These discrepancies can be due to local effects related to the bathymetry that we are not able to reproduce at the resolution used in this study.

A summary of the statistical results obtained for both data set (GOS 1.1 and GOS 2.1) is shown in Table 1. The RMSE and the correlation index are presented for each tide-gauge station. The information gathered in this table is also presented in Figs. 5 and 6, where the spatial comparison between the model output and in situ measurements is shown. Figure 5 corresponds to the correlation coefficient (ρ) while Fig. 6 represents the RMSE. A good agreement between measured and numerical data is obtained at all locations, except for those tide gauges placed in the Northern Adriatic (stations of Trieste, Venezia, Ravenna and Ancona). As displayed in Table 1, GOS 2.1 achieves slightly higher correlation coefficients and slightly smaller errors than GOS 1.1 although it still does not represent correctly storm surge in the Northern Adriatic. Models in general have difficulty in reproducing sea level in the Adriatic (Marcos et al. 2009). The results found in the northern part of the Adriatic Sea can probably be explained in terms of the relatively shallow shelf present in this area, which makes extremely important the use of an accurate frictional parameter as well as a high resolution bathymetry, aspects that greatly affect the model results. Similar explanation was found by Pascual et al. (2008) in the Northern Adriatic area. Another issue is the Meteorological tsunamis that can affect the Northern Adriatic

(Šepić et al. 2012). They are very difficult to accurately reproduce since a very high spatial–temporal resolution and precise forcing are required to obtain good simulations. Except for these stations, results show a good agreement between measured and numerical data. In terms of correlation (see Table 1; Fig. 5), high correlation indices are obtained between numerical and observed data for both data set. In the Atlantic area, the correlation factor is over 0.8 (over 0.85 in the stations placed along the north coast of Spain), while the correlation found in the Mediterranean Sea is about 0.75. The whole set of tide gauge data (58 stations) has a RMSE lower or around 10 cm (see Table 1; Fig. 6). These RMSE represent around the 10 % of the storm surge variability registered by the tide gauge, which shows the accuracy of the hindcasts performed. These results are similar to the ones found in previous studies (Ratsimandresy et al. 2008), where the highest correlations (over 0.85) are observed in the tide gauges moored along the north and northwest coast of the Iberian Peninsula.

Differences between numerical and observed surge should exist since the signals gathered in each series do not take into account the same processes. While sea level variation in the model is strictly due to wind and pressure, in tide gauges there are local factors or processes (as steric effects, the influence of river outflow, the effects of waves in storm surge or non-linear interactions between storm surge and tides) that have not been considered in this study.

The statistical validation shows similar results for both storm surge data set. Although GOS 2.1 achieves slightly higher correlation coefficients and slightly smaller errors than GOS 1.1, in general the results show no significant improvements when increasing the resolution of the atmospheric forcing fields from 30 to 15 km. Thus, in this work, the increase of the atmospheric forcing resolution

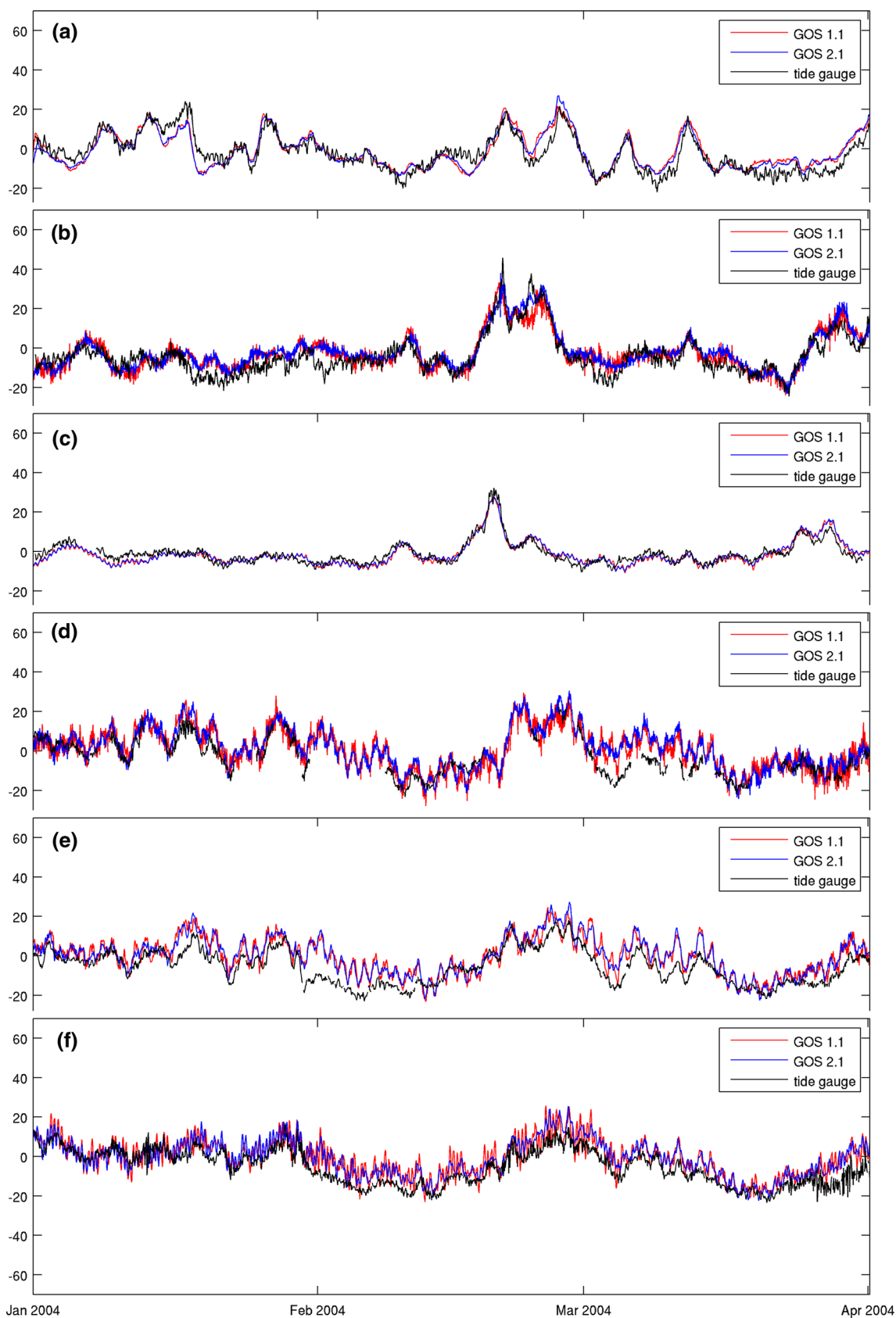


Fig. 3 Storm surge comparison between model (GOS 1.1 in red and GOS 2.1 in blue) and tide gauge (grey) at six locations. **a** Santander, **b** Huelva, **c** Arinaga, **d** Genova, **e** Porto Torres, **f** Palermo

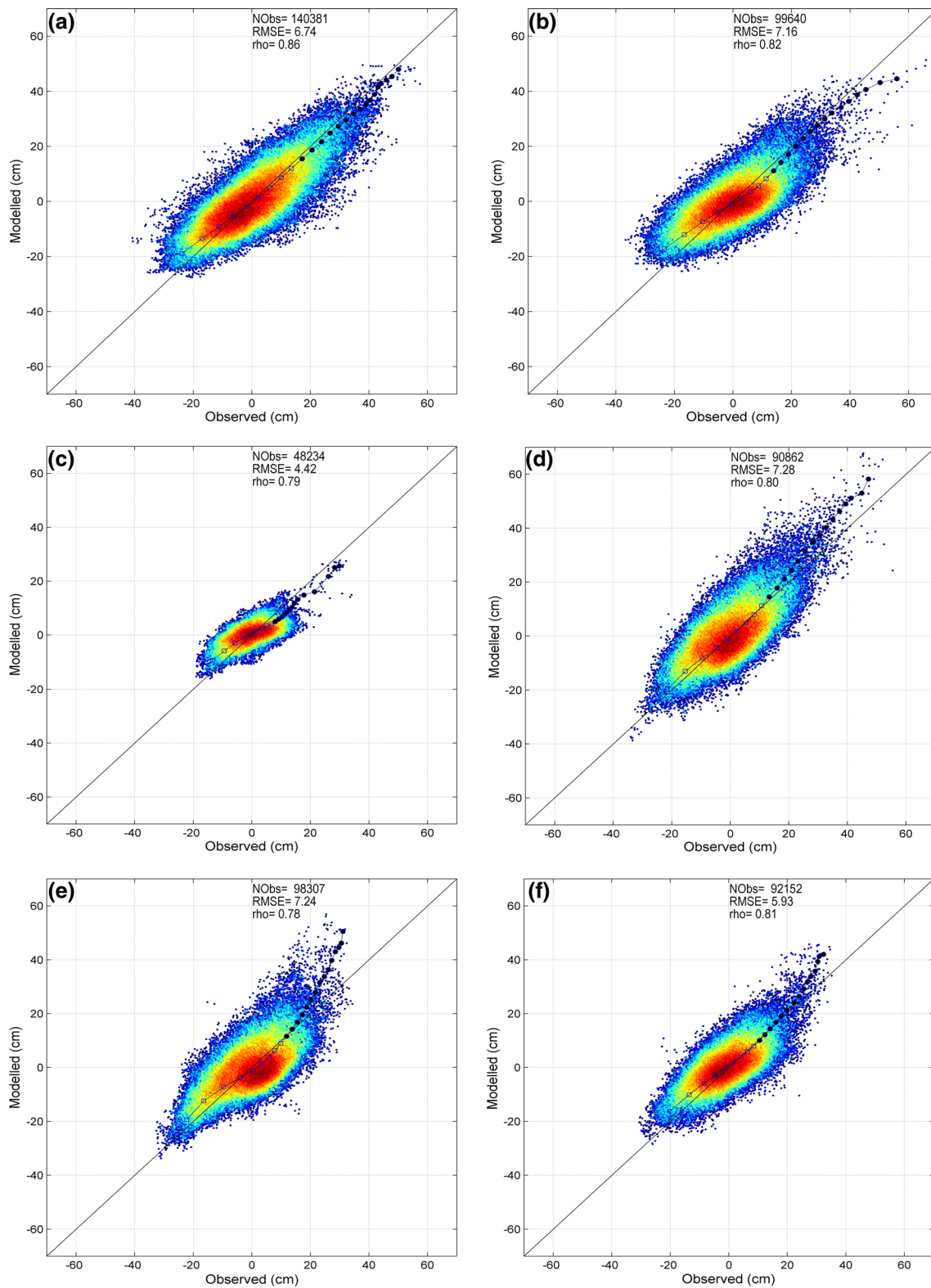


Fig. 4 Diagnosis comparison between 6 tide gauges and GOS 2.1 dataset. Quantiles (*solid circles* are quantiles over the 90th percentiles) and statistical indices of observed versus modelled values are

shown. *Colours* represent data density (increasing values from *blue* to *red*) **a** Santander, **b** Huelva, **c** Arinaga, **d** Genova, **e** Porto Torres, **f** Palermo

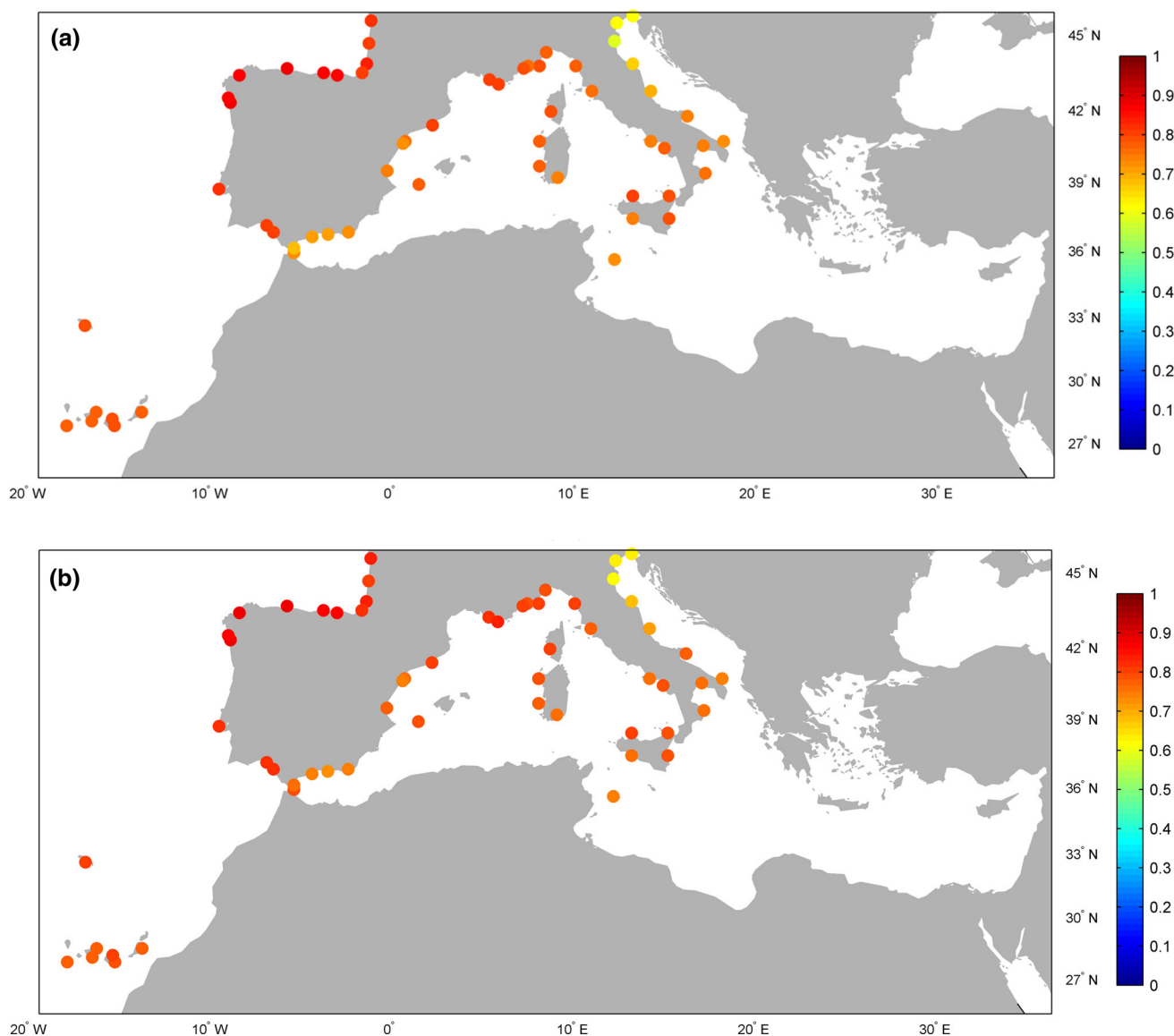


Fig. 5 Comparisons of the storm surge dataset with in situ measurements in terms of correlation index (ρ) **a** GOS 1.1, **b** GOS 2.1

has negligible effect in the storm surge sea level. Nevertheless, a further analysis should be performed in order to study how the increase of the forcing resolution affects the storm surge results at the local scale (e.g. coastal areas, estuaries or bays).

3.2 Satellite altimetry versus modelled data

Additionally, GOS hindcasts are compared to satellite information for the whole spatial domain. This is motivated by the sparse distribution of tide gauges along the analysed coastline and the need of evaluating the model on the open ocean.

The altimeter data used in this study are along-track delayed time products. These data were produced by Ssalto/

Duacs and distributed by Aviso, with support from Cnes (<http://www.aviso.oceanobs.com/duacs/>). The Delayed Time component of Ssalto/Duacs system provides a homogeneous, inter-calibrated and highly accurate long time series of SLA altimetry data from T/P, ERS1/2, GFO, Envisat, Jason-1 and Jason-2 missions. These satellite time series started in 1992 and they are constantly updated. The minimum time lapse of the satellites is around 10 days.

The sea level anomaly (SLA) currently delivered has the classical geophysical and instrumental corrections, including instrumental noise, orbit determination error, atmospheric attenuation (wet and dry tropospheric and ionospheric effects), and sea state bias (more information in “User Handbook Ssalto/Duacs: M(SLA) and M(ADT) Near-Real Time and Delayed-Time”). Tides were removed

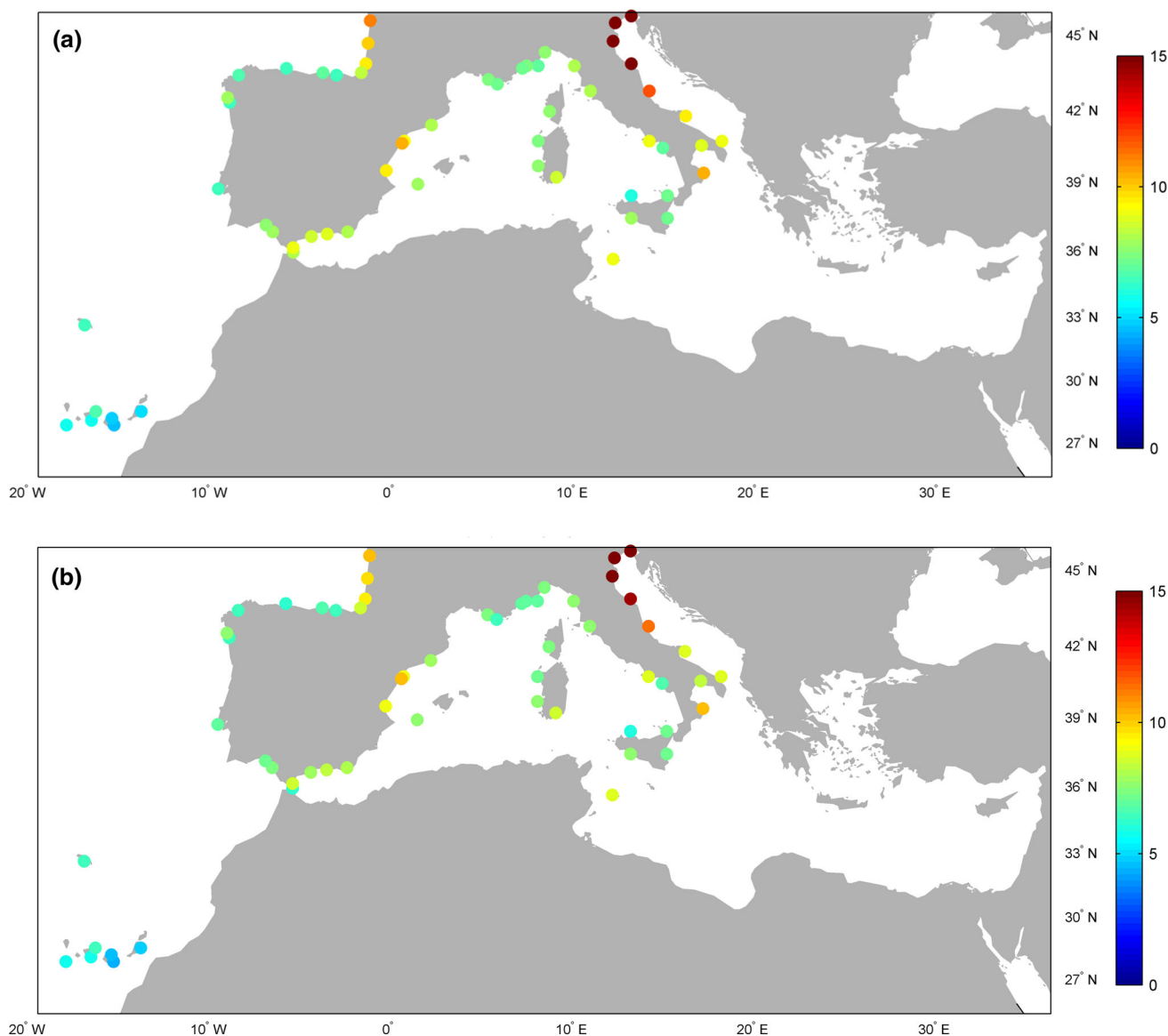


Fig. 6 Comparisons of the storm surge dataset with in situ measurements in terms of root mean square error (RMSE). Units are in centimetres. **a** GOS 1.1, **b** GOS 2.1

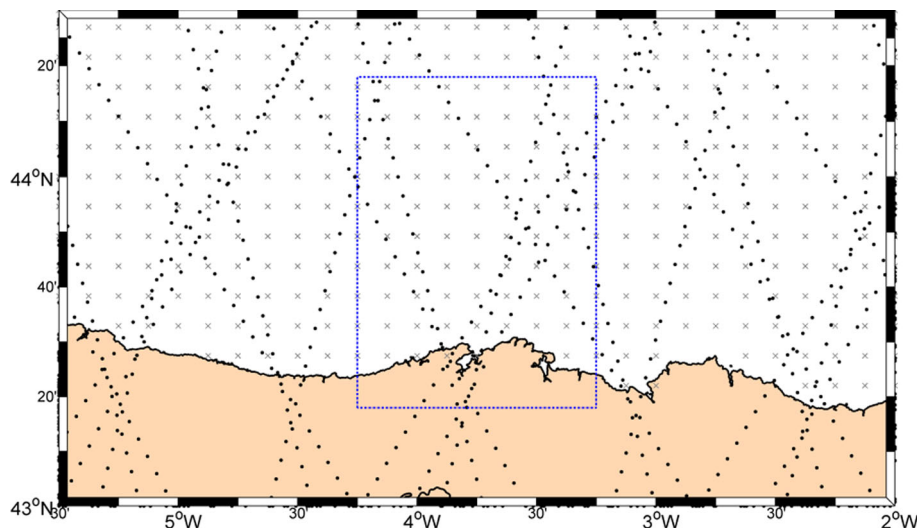
using GOT4.8 tidal model (Ray 1999). High-frequency signals were also corrected using a combination of a hydrodynamic model (MOG2D-G) for high frequencies (Carrère 2003) and an inverse barometer (IB) for low frequencies, therefore the sea level variation due to atmospheric forcing is not included in the delivered SLA. However, these high-frequency signals are also delivered under the name of Dynamic Atmospheric Correction (DAC) as an auxiliary product (Dynamic Atmospheric Corrections are produced by CLS Space Oceanography Division using the Mog2D model from Legos and distributed by Aviso, with support from Cnes, <http://www.avisio.oceanobs.com/>). This product is currently used in the correction of the altimeter data sets in order to reduce the

aliasing effects of high frequency signals (Volkov et al. 2007). In this work, in order to have the sea level variation due to atmospheric forcing included in the altimeter data, DAC product has been added to the along-track DT-SLA (Delayed Time Sea Level Anomaly).

Once the along-track satellite data has the sea level variation due to atmospheric forcing included, the domain is divided in 1-by-1 degree boxes. At each box, all the satellite data placed within it are selected and compared with the closest grid point (in space and time) from GOS database, an example is shown in Fig. 7.

In order to compare model outputs and satellite data, a statistical analysis is carried out for each box. Since satellite data start in 1992 and the hindcast database ends

Fig. 7 Along-track satellite measures (*black points*) within a 1-by-1 degree box centred in Santander (Spain). *Grey crosses* represent GOS grid nodes



up in 2009, a period between 1992 and 2009 is selected to perform the validation. The comparison with satellite data is made for both databases. Here the results for GOS 2.1 are presented. The validation of GOS 1.1 provides very similar results (not shown).

An example of some scatterplots, performed for the areas that overlap the tide gauge locations presented in Fig. 4, can be seen in Fig. 8. They show the comparison between the satellite and GOS results, taking into account all the data within a 1-by-1 degree box centred at the tide gauge position. Contrasting these scatterplots with the ones obtained from the tide gauge validation (see Fig. 4), slight differences in RMSE and ρ can be observed, as well as a steeper underestimation of the results. It should be kept in mind that the number of available satellite data is considerably smaller than the tide gauge observations. Therefore, the validation with altimeters is also accurate, as shown in Fig. 9, where the correlation factor and the RMSE are displayed. These results show a good agreement between the model output and the satellite data. The correlation factor is high through most of the domain (>0.75) except for three areas: Northern Adriatic, Aegean Sea and Gulf of Gabes. Similar to the already discussed case of the North Adriatic, also for these other two shallow semi-enclosed basins, the less accurate results could be related to limitations in data available (e.g., bathymetry) or description of physical processes (e.g., friction). Lower RMSE are found in the Atlantic, where the maximum discrepancy is around 8 cm. In the Mediterranean Sea, apart from the three areas above mentioned, the highest errors observed are about 10 cm. Authors as Marcos and Tsimplis (2007) or García-Lafuente et al. (2004) have suggested that the steric signal may be higher in the Mediterranean than in the Atlantic; this would explain the differences in the RMSE found between the two areas.

Validation with altimeter data has shown the good accuracy of GOS database. As was already mentioned in Sect. 3.1, even though modelled series and satellite series do not include sea level variations due to exactly the same forcings, high correlations and low errors are obtained from this comparison.

Validation with altimeters has allowed the identification of some areas where GOS databases do not represent correctly the storm surge level. In these regions, GOS signal overestimates altimeter data. If the reason of these differences lied in an inadequate spatial resolution of the atmospheric forcing, storm surge results should lead to an underestimation of the signal, as pointed out by Wakelin and Proctor (2002), where they conclude that a coarse spatial resolution in the atmospheric forcing results in an underestimation of the amplitude of the surges in the Adriatic Sea. Hence, the overestimation of GOS in these relatively shallow areas, could be more probably explained in terms of the bathymetry or frictional parameters used, as already suggested by Pascual et al. (2008).

4 Storm surge variability

In this section, long term variability and trends in storm surge are calculated using GOS databases. For this purpose time series at each grid point are averaged at different time scales. Averages are made monthly and seasonally, and trends are obtained by a linear fit to each grid point.

Some studies carried out so far (Tsimplis et al. 2005; Gomis et al. 2008; Calafat and Gomis 2009) have pointed out the different results obtained when computing trends from different periods. For this reason, according to the developed GOS data set, the storm surge behaviour for two time periods is investigated. A long term trend from 1948

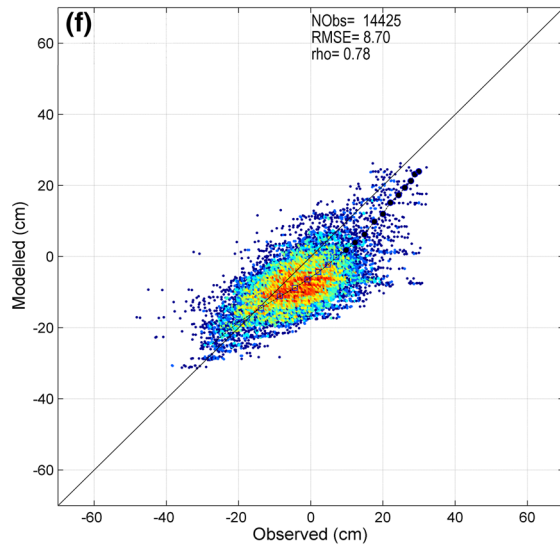
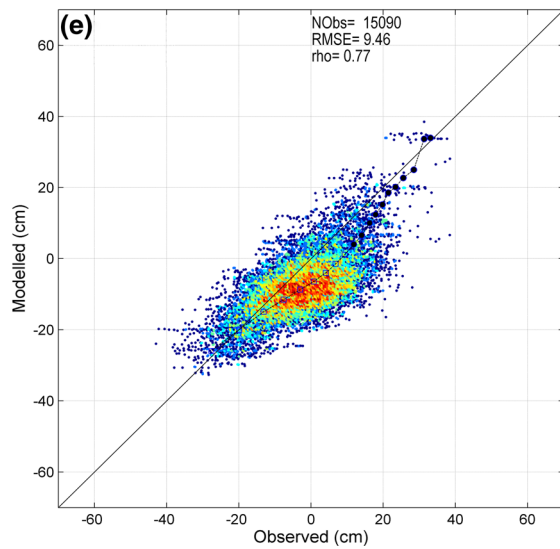
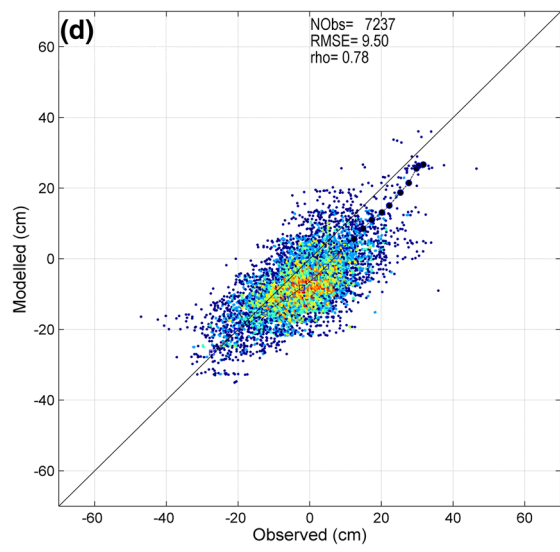
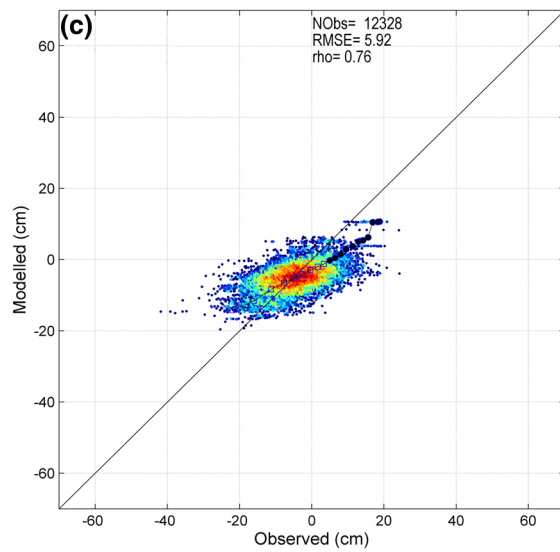
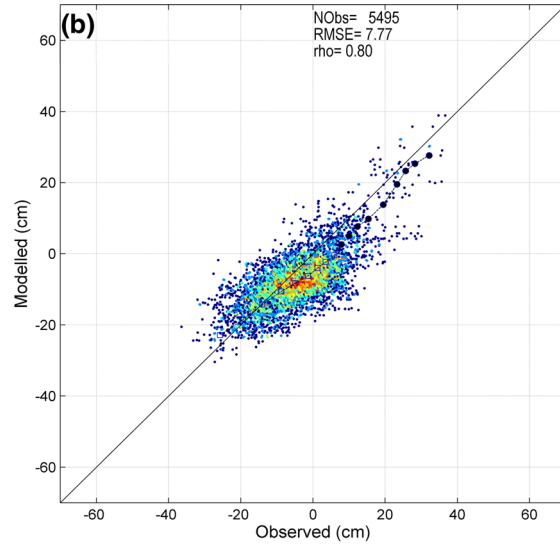
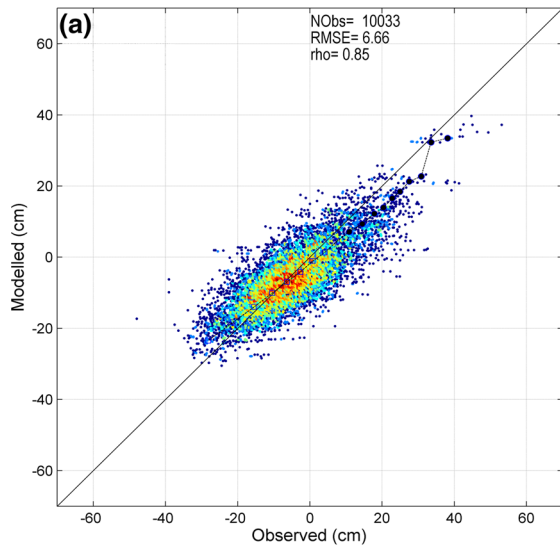


Fig. 8 Diagnostics plots for the 1-by1 degree boxes associated with tide gauges from Fig. 4 used for the validation of GOS 2.1 dataset. Quantiles (solid circles are quantiles over the 90th percentiles) and statistical indices of observed versus modelled values are shown. Colours represent data density (increasing values from blue to red). **a** Santander, **b** Huelva, **c** Arinaga, **d** Genova, **e** Porto Torres, **f** Palermo

to 2009, and a recent trend from 1989 to 2009, are estimated. Storm surge trends for the last 61 years (GOS 1.1) and for the last 21 years (GOS 2.1) are presented in Fig. 10. The analysis for the last two decades was also done using GOS 1.1; trends are similar (not shown) to the ones obtained with GOS 2.1 (Fig. 10b), suggesting that trends do not depend on the database but on the period analysed. Trends for the 1948–2009 period (Fig. 10a) are negative in all domain, showing stronger values in the

Atlantic African coast, the Adriatic and the North-East of the Levantine basin, with values around -0.35 mm/year. Weaker trends are found in the North Atlantic Spanish coast and also along the East part of the Mediterranean African coast, where trends are about -0.1 mm/year. Figure 10b shows trends for the 1989–2009 period, in this case trends are positive all along the domain, showing quite uniform values around 0.5 mm/year for the Atlantic sector and more variability in the Mediterranean Sea with values ranging between 0.6 and 1.5 mm/year. Similar results were obtained by Gomis et al. (2008) when computing trends for modelled sea level due to wind and pressure. They showed negative values when computing trends for period 1958–2001 and positive values when computing trends for period 1993–2001. This difference in the sign of the trends also found between GOS 1.1 (1948–2009) and GOS 2.1

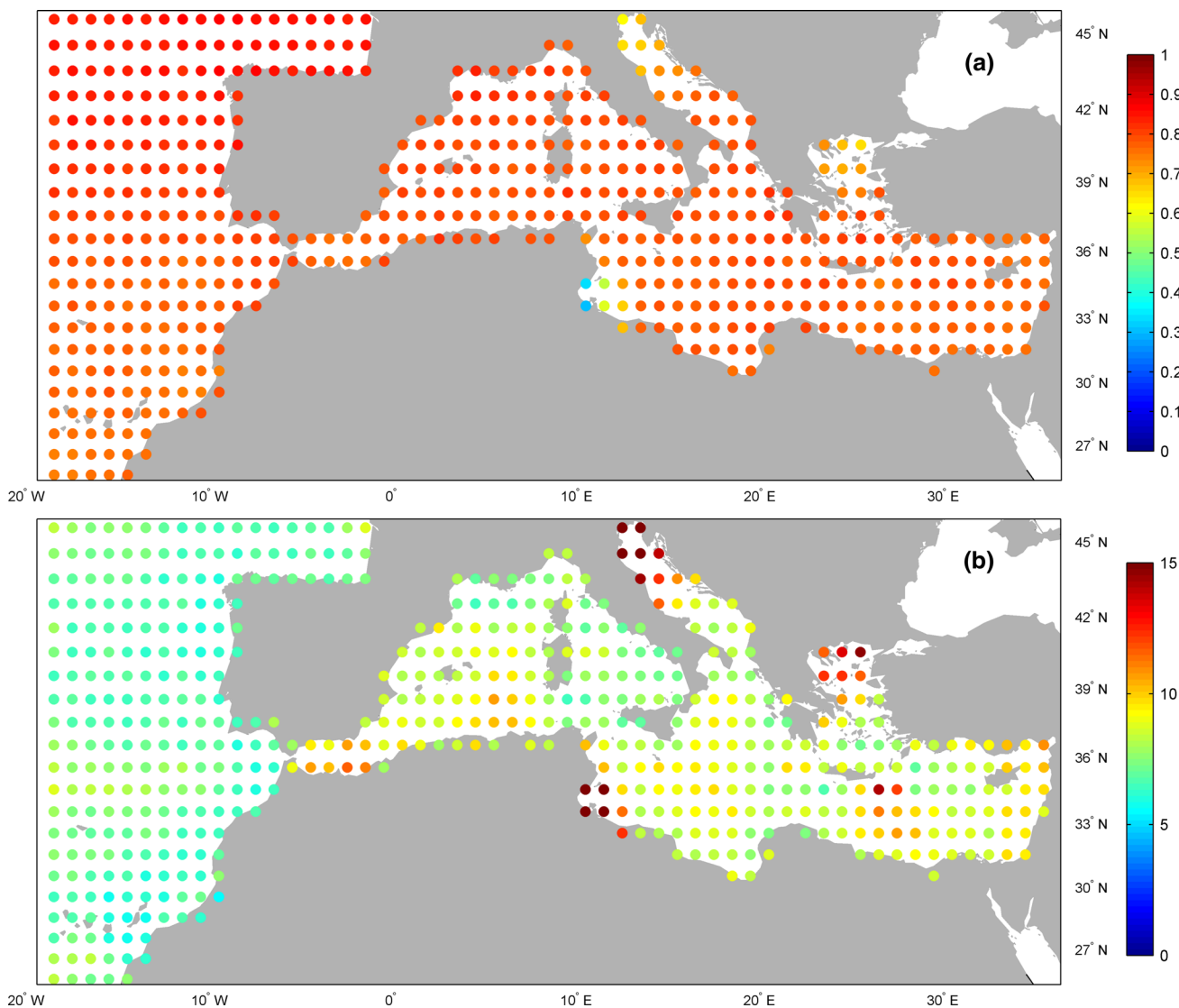


Fig. 9 Comparison between GOS 2.1 hindcast and altimeter data. **a** Correlation index (ρ), **b** Root mean square error in cm (RMSE)

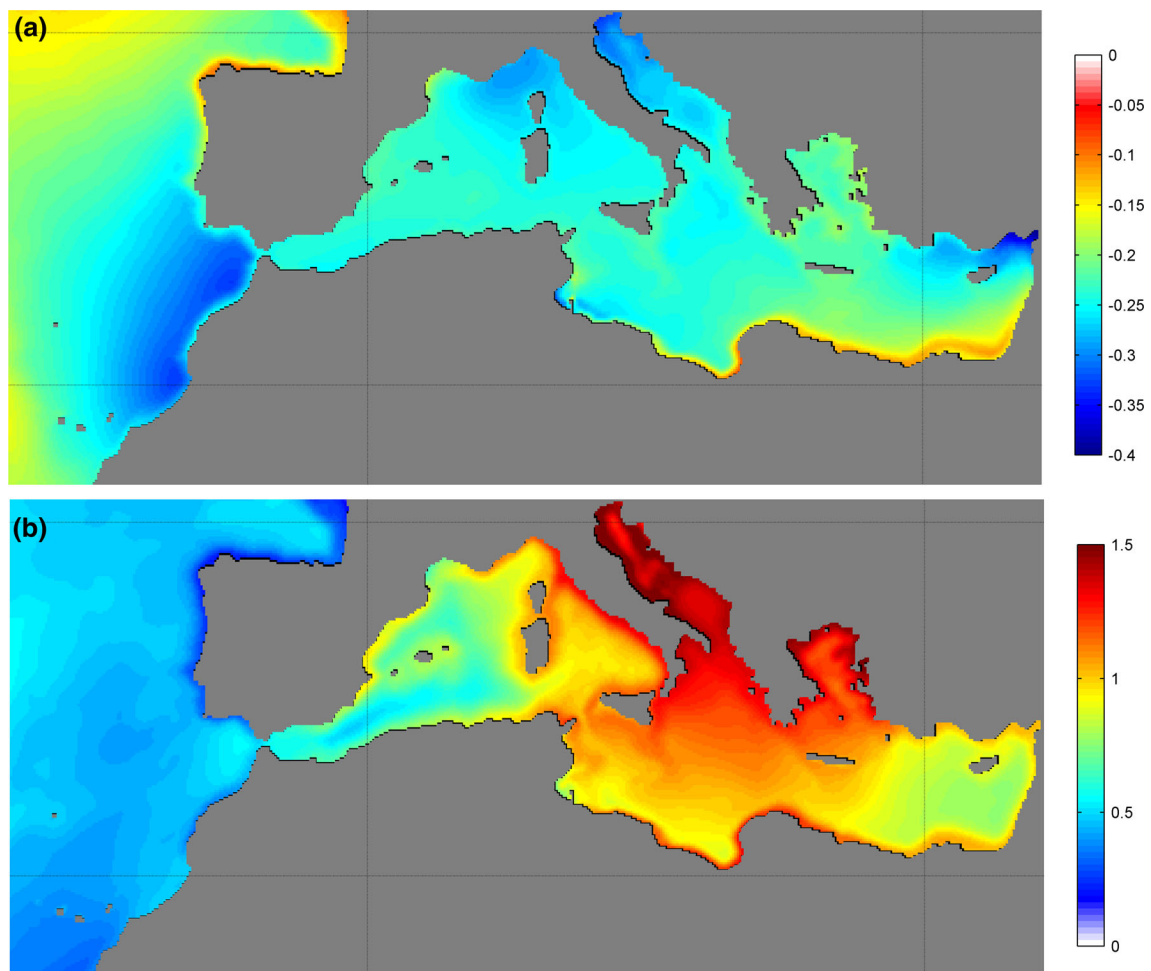


Fig. 10 **a** Estimated long term trends (mm/year) of storm surge for GOS 1.1 (1948–2009) and **b** estimated trend (mm/year) for the last two decades (1989–2009, GOS 2.1)

(1989–2009) can be correlated with trends obtained from tide gauges by Tsimplis and Baker (2000) and Tsimplis et al. (2005). They displayed negative trends for the period 1960–1994 in most of the Mediterranean tide gauges (typically between -0.5 and -1 mm/year), while for the last decade tide gauges reported sea level trends between $+5$ and $+10$ mm/year. Therefore, trends in the observed sea level could be partially explained in terms of changes in the atmospheric forcing.

To analyse seasonal variability of storm surge, hourly series are averaged gathering each season of every year in a single value. Periods are defined as: Spring (March 15th–June 15th), summer (June 15th–September 15th), autumn (September 15th–December 15th), and winter (December 15th–March 15th). Figure 11 shows mean values for each season for GOS 1.1. As can be seen, the transitional stages, spring and autumn, show a weak climate variability of mean storm surge, with quite uniform values ranging between -1 and $+1$ cm in most of the domain. Summer

and winter present an opposite spatial pattern to each other. In summer, highest values are found in the Eastern Mediterranean basin (~ 3 cm) and slightly smaller along the African Atlantic coast. Lowest values are found in the Adriatic, North Atlantic Spanish coast and Libya and Tunisia coasts (~ -3 cm). Highest mean storm surge levels during winter season are located at the Gulf of Biscay, north coast of the Iberian Peninsula, the whole Italian coast and the Adriatic Sea and also along the eastern Mediterranean African coast and the Aegean Sea.

Figure 12 shows the seasonal trends for winter and summer periods. As can be observed, winter trends are negative all along the domain. Strong trends are found in the Adriatic and in the central Mediterranean, with values around -1 mm/year. Smaller but still negative trends are found in the Eastern Mediterranean and in the Atlantic area. Summer trends show positive and negative values. Positive values of around 0.1 mm/year are found in the North Atlantic and Mediterranean Spanish coast and also

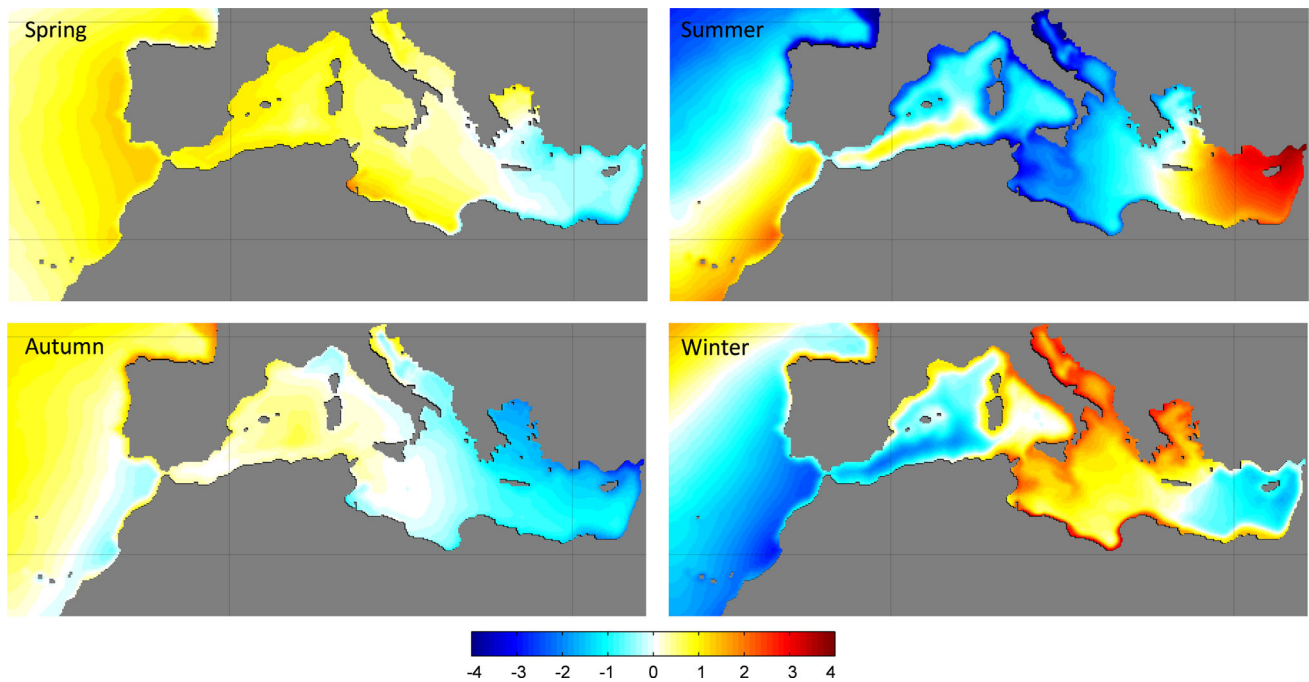


Fig. 11 Mean seasonal values of storm surge (cm) for the 1948–2009 period (GOS 1.1)

along the Tunisian coast. The strongest negative trends (~ -0.3 mm/year) are found along the Atlantic African coast. Similar patterns regarding seasonal trends were found by Gomis et al. (2008).

5 Summary and conclusions

The main objective of this study was the generation of a long-term high-resolution ($1/8^\circ$) storm surge database for Southern Europe. Studying the sensitivity of the storm surge results to the resolution of the atmospheric fields was also possible through the two different runs carried out using ROMS model. The difference between the two hindcasts lies in the atmospheric forcing used. These atmospheric fields were the result of two dynamical downscalings: a regional re-forecast coupling the WRF-ARW model to NCEP reanalysis and to ERA-Interim conditions. The model is driven hourly with these high-resolution atmospheric fields (30 and 15 km, respectively). Therefore, two hourly data set of storm surge hindcast are obtained: GOS 1.1, a 62-year (1948–2009) dataset forced with an atmospheric downscaling (30 km) obtained with NCEP reanalysis; and GOS 2.1 a 21-year (1989–2009) dataset forced with an atmospheric downscaling (15 km) obtained with ERA-Interim.

The storm surge numerical results are comprehensively validated using data provided by tide gauges and altimeter data distributed throughout the domain. It is worthy to note

that: (1) 58 tide gauges are used for the validation; (2) validation with satellite data has allowed a wide spatial comparison. The spatial validation has pointed out some areas where the model shows unreliable results that otherwise would have not been noticed due to the lack of tide gauges measures in those areas. The overestimation of the model in these relative shallow and semi-enclosed areas could be explained in terms of the bathymetry or the frictional parameters used. However, a further study is needed in order to address other possible sources (e.g., resonance of the surges).

The statistical analysis carried out shows that, at tide gauge locations, the correlation factor is over 0.8 in the Atlantic area and about 0.75 in the Mediterranean Sea. RMSE are lower or around 10 cm for the whole set of tide gauges.

Accurate results are also obtained when comparing with satellite data. Most of the domain presents a correlation index over 0.75 and a RMSE of 8–10 cm. This validation has shown the good agreement between modelled and measured data and the capability of the model to simulate accurately storm surge sea level.

Regarding the sensitivity of the storm surge results to the resolution of the atmospheric fields, the statistical validation shows similar results for both storm surge data set GOS 1.1 and GOS 2.1. Although the correlation coefficients are slightly higher for GOS 2.1, the results show no significant improvement when increasing the resolution of the atmospheric forcing fields from 30 to 15 km. We

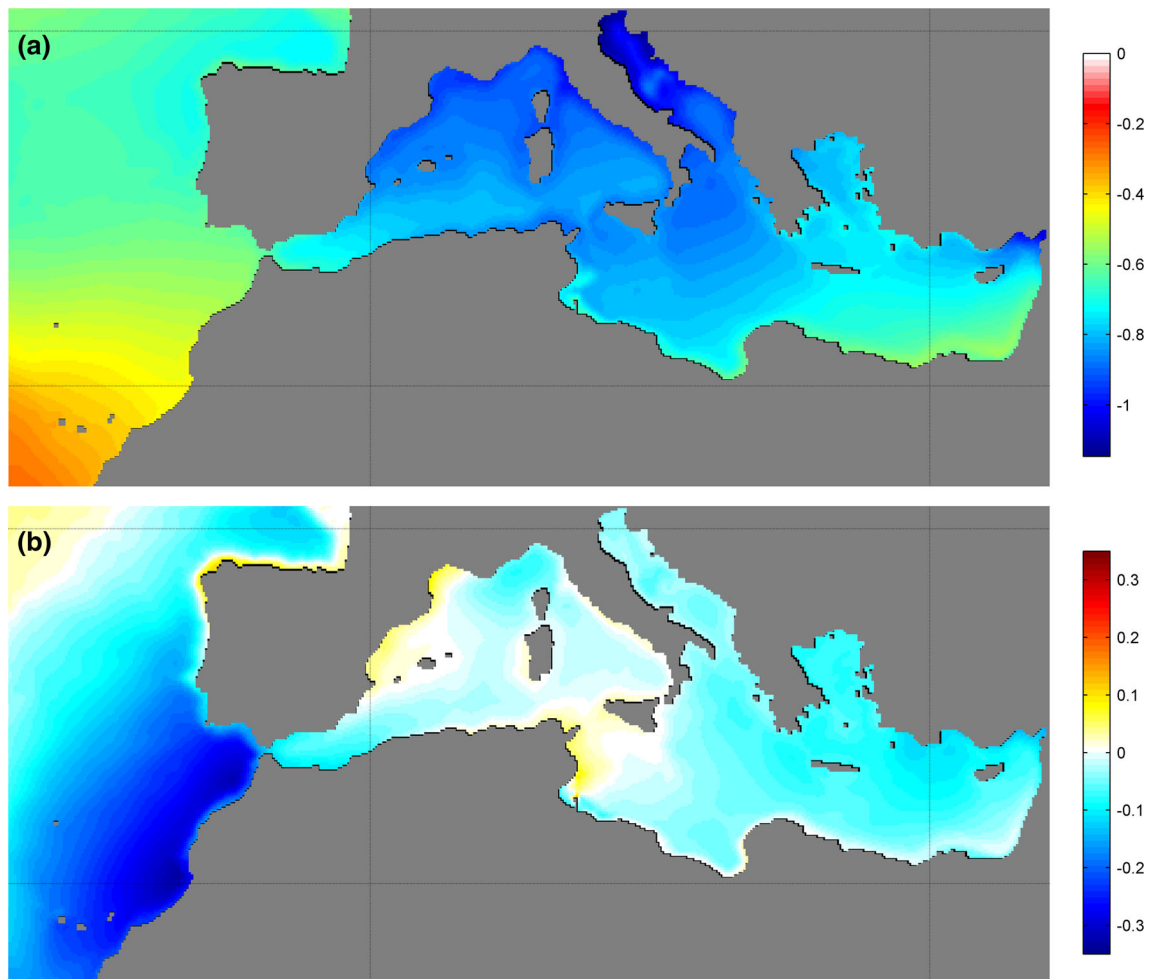


Fig. 12 Seasonal trends (mm/year) for the 1948–2009 period (GOS 1.1). **a** Winter, **b** Summer

should bear in mind that both atmospheric forcings are already high-resolution fields and both have an hourly temporal resolution, thus differences between the two GOS databases should not be as noticeable as the ones found by other authors (Wakelin and Proctor 2002) since they compared data with really different temporal and spatial resolutions. Moreover, a further analysis in coastal or estuarine areas should be carried out in order to test how increasing the atmospheric forcing resolution affects the results at local scale.

The analysis of the storm surge variability has identified negative trends for the period 1948–2009 (GOS 1.1) while positive trends are obtained for the last 20 years (GOS 2.1). These results are in agreement with trends found in Mediterranean tide gauges by Tsimplis et al. (2005) and with trends from a numerical model found by Gomis et al. (2008), showing that trends are positive before 1960 and also during the period 1993–2001, while during 1960–1994 sea level trends are negative. The seasonal analysis has also

shown that the overall negative trends found in the domain are mainly driven by the winter season.

This work has shown how the new storm surge database can be applied to study variability and trends. Future studies could use the databases to address for example extreme events. Further improvements in terms of bathymetry resolution and, possibly, a downscaling at coastal scale could provide insight on local processes and improve predictability.

Acknowledgments The authors would like to thank Puertos del Estado for the REDMAR network's data provided for this study, as well as the University of Hawaii Sea Level Center, Système d'Observation du Niveau des Eaux Littorales and Istituto Superiore per la Protezione e la Ricerca Ambientale. The satellite data were produced by Ssalto/Duacs and distributed by Aviso, with support from Cnes. This work was partly funded by the Projects iMar21 (CTM2010-15009) and SaltyCor (BIA2011-29031-C02-00) from the Spanish government, and from the FP7 European Projects CoCoNet (287844) and Theseus (ENV.2009-1, n244104). GOS 1.1 and GOS 2.1 data sets are available under request for scientific purposes.

References

- Backhaus JO (1985) A three-dimensional model for the simulation of shelf sea dynamics. *Deutsche Hydrographische Zeitschrift* 38:165–187. doi:[10.1007/BF02328975](https://doi.org/10.1007/BF02328975)
- Bernier NB, Thompson KR (2006) Predicting the frequency of storm surges and extreme sea levels in the northwest Atlantic. *J Geophys Res* 111:C10009. doi:[10.1029/2005JC003168](https://doi.org/10.1029/2005JC003168)
- Brown JM, Souza AJ, Wolf J (2010) An 11-year validation of wave-surge modelling in the Irish Sea, using a nested POLCOMS–WAM modelling system. *Ocean Model* 33:118–128. doi:[10.1016/j.ocemod.2009.12.006](https://doi.org/10.1016/j.ocemod.2009.12.006)
- Butler A, Heffernan JE, Tawn JA et al (2007) Extreme value analysis of decadal variations in storm surge elevations. *J Mar Syst* 67:189–200. doi:[10.1016/j.jmarsys.2006.10.006](https://doi.org/10.1016/j.jmarsys.2006.10.006)
- Calafat FM, Gomis D (2009) Reconstruction of Mediterranean sea level fields for the period 1945–2000. *Global Planet Change* 66:225–234. doi:[10.1016/j.gloplacha.2008.12.015](https://doi.org/10.1016/j.gloplacha.2008.12.015)
- Carrère L (2003) Modeling the barotropic response of the global ocean to atmospheric wind and pressure forcing—comparisons with observations. *Geophys Res Lett* 30:1275. doi:[10.1029/2002GL016473](https://doi.org/10.1029/2002GL016473)
- Carretero JC, Alvarez Fanjul E, Gómez Lahoz M et al (2000) Ocean forecasting in narrow shelf seas: application to the Spanish coasts. *Coast Eng* 41:269–293. doi:[10.1016/S0378-3839\(00\)00035-1](https://doi.org/10.1016/S0378-3839(00)00035-1)
- Dee DP, Uppala SM, Simmons AJ et al (2011) The ERA-Interim reanalysis: configuration and performance of the data assimilation system. *Q J R Meteorol Soc* 137:553–597. doi:[10.1002/qj.828](https://doi.org/10.1002/qj.828)
- Ferrarin C, Roland A, Bajo M, Umgiesser G, Cucco A, Davolio S, Drofa O (2013) Tide-surge-wave modelling and forecasting in the Mediterranean Sea with focus on the Italian coast. *Ocean Model* 61(2):38–48. doi:[10.1016/j.ocemod.2012.10.003](https://doi.org/10.1016/j.ocemod.2012.10.003)
- Flather R, Williams J (2000) Climate change effects on storm surges: methodologies and results. *ECLAT-2 Workshop* 66–78
- Flather RA, Smith JA, Richards JD et al (1998) Direct estimates of extreme storm surge elevations from a 40-year numerical model simulation and from observations. *Glob Atmos Ocean Syst* 6:165–176
- García-Lafuente J, Del Río J, Alvarez Fanjul E, et al (2004) Some aspects of the seasonal sea level variations around Spain. *J Geophys Res* 109. doi:[10.1029/2003JC002070](https://doi.org/10.1029/2003JC002070)
- Gomis D, Ruiz S, Sotillo MG et al (2008) Low frequency Mediterranean sea level variability: the contribution of atmospheric pressure and wind. *Global Planet Change* 63:215–229. doi:[10.1016/j.gloplacha.2008.06.005](https://doi.org/10.1016/j.gloplacha.2008.06.005)
- Haidvogel DB, Arango HG, Hedstrom K et al (2000) Model evaluation experiments in the North Atlantic Basin: simulations in nonlinear terrain-following coordinates. *Dyn Atmos Oceans* 32:239–281. doi:[10.1016/S0377-0265\(00\)00049-X](https://doi.org/10.1016/S0377-0265(00)00049-X)
- Haidvogel DB, Arango H, Budgell WP et al (2008) Ocean forecasting in terrain-following coordinates: formulation and skill assessment of the regional Ocean modeling system. *J Comput Phys* 227:3595–3624. doi:[10.1016/j.jcp.2007.06.016](https://doi.org/10.1016/j.jcp.2007.06.016)
- Jacob D, Podzun R (1997) Sensitivity studies with the regional climate model REMO. *Meteorol Atmos Phys* 63:119–129. doi:[10.1007/BF01025368](https://doi.org/10.1007/BF01025368)
- Jones EJ, Davies AM (2006) Application of a finite element model (TELEMAC) to computing the wind induced response of the Irish Sea. *Cont Shelf Res* 26:1519–1541. doi:[10.1016/j.csr.2006.03.013](https://doi.org/10.1016/j.csr.2006.03.013)
- Jordà G, Gomis D, Álvarez-Fanjul E, Somot S (2012) Atmospheric contribution to Mediterranean and nearby Atlantic sea level variability under different climate change scenarios. *Global Planet Change* 80–81:198–214. doi:[10.1016/j.gloplacha.2011.10.013](https://doi.org/10.1016/j.gloplacha.2011.10.013)
- Kalnay E, Kanamitsu M, Kistler R et al (1996) The NCEP/NCAR 40-year reanalysis project. *Bull Am Meteorol Soc* 77:437–471. doi:[10.1175/1520-0477\(1996\)077<0437:TNYRP>2.0.CO;2](https://doi.org/10.1175/1520-0477(1996)077<0437:TNYRP>2.0.CO;2)
- Lionello P (2012) The climate of the Mediterranean region from the past to the future, 1st Edition 592
- Losada IJ, Reguero BG, Méndez FJ, Castanedo S, Abascal AJ, Mínguez R (2013) Long-term changes in sea-level components in Latin America and the Caribbean. *Global Planet Change* 104:34–50
- Lowe JA, Gregory JM, Flather RA (2001) Changes in the occurrence of storm surges around the United Kingdom under a future climate scenario using a dynamic storm surge model driven by the Hadley Centre climate models. *Clim Dyn* 18:179–188. doi:[10.1007/s003820100163](https://doi.org/10.1007/s003820100163)
- Marcos M, Tsimplis MN (2007) Variations of the seasonal sea level cycle in southern Europe. *J Geophys Res* 112:2007
- Marcos M, Tsimplis MN, Shaw AGP (2009) Sea level extremes in southern Europe. *J Geophys Res* 114:1–16. doi:[10.1029/2008JC004912](https://doi.org/10.1029/2008JC004912)
- Menéndez M, García-Díez M, Fita L et al (2013) High-resolution sea wind hindcasts over the Mediterranean area. *Clim Dyn*. doi:[10.1007/s00382-013-1912-8](https://doi.org/10.1007/s00382-013-1912-8)
- Pascual A, Marcos M, Gomis D (2008) Comparing the sea level response to pressure and wind forcing of two barotropic models: validation with tide gauge and altimetry data. *J Geophys Res* 113:C07011. doi:[10.1029/2007JC004459](https://doi.org/10.1029/2007JC004459)
- Pawlowicz R, Beardsley B, Lentz S (2002) Classical tidal harmonic analysis including error estimates in MATLAB using T_TIDE. *Comput Geosci* 28:929–937. doi:[10.1016/S0098-3004\(02\)00013-4](https://doi.org/10.1016/S0098-3004(02)00013-4)
- Ratsimandresy AW, Sotillo MG, Carretero Albiach JC et al (2008) A 44-year high-resolution ocean and atmospheric hindcast for the Mediterranean Basin developed within the HIPOCAS Project. *Coast Eng* 55:827–842. doi:[10.1016/j.coastaleng.2008.02.025](https://doi.org/10.1016/j.coastaleng.2008.02.025)
- Ray R (1999) A global Ocean tide model from TOPEX/Poseidon altimetry: GOT99.2. NASA Technical Memo 1999–209478
- Sebastião P, Guedes Soares C, Alvarez E (2008) 44 years hindcast of sea level in the Atlantic coast of Europe. *Coast Eng* 55:843–848. doi:[10.1016/j.coastaleng.2008.02.022](https://doi.org/10.1016/j.coastaleng.2008.02.022)
- Šepić J, Vilibić I, Strelec Mahović N (2012) Northern Adriatic meteorological tsunamis: observations, link to the atmosphere, and predictability. *J Geophys Res* 117(C2):C02002. doi:[10.1029/2011JC007608](https://doi.org/10.1029/2011JC007608)
- Shchepetkin AF, McWilliams JC (2005) The regional oceanic modeling system (ROMS): a split-explicit, free-surface, topography-following-coordinate oceanic model. *Ocean Model* 9:347–404. doi:[10.1016/j.ocemod.2004.08.002](https://doi.org/10.1016/j.ocemod.2004.08.002)
- Skamarock WC, Klemp JB, Dudhia J et al (2008) A description of the advanced research WRF version 3. In: NCAR Technology, NCAR/TN- 475+ STR
- Smith WH, Sandwell DT (1997) Global Sea floor topography from satellite altimetry and ship depth soundings. *Science* 277:1956–1962. doi:[10.1126/science.277.5334.1956](https://doi.org/10.1126/science.277.5334.1956)
- Tsimplis MN, Baker TF (2000) Sea level drop in the Mediterranean Sea: an indicator of deep water salinity and temperature changes? *Geophys Res Lett* 27:1731–1734
- Tsimplis MN, Alvarez-Fanjul E, Gomis D et al (2005) Mediterranean Sea level trends: atmospheric pressure and wind contribution. *Geophys Res Lett* 32:L20602. doi:[10.1029/2005GL023867](https://doi.org/10.1029/2005GL023867)
- Volkov DL, Larnicol G, Dorandeu J (2007) Improving the quality of satellite altimetry data over continental shelves. *J Geophys Res* 112:C06020. doi:[10.1029/2006JC003765](https://doi.org/10.1029/2006JC003765)
- Wakelin S, Proctor R (2002) The impact of meteorology on modelling storm surges in the Adriatic Sea. *Global Planet Change* 34:97–119

- Wang S, McGrath R, Hanafin J et al (2008) The impact of climate change on storm surges over Irish waters. *Ocean Model* 25:83–94. doi:[10.1016/j.ocemod.2008.06.009](https://doi.org/10.1016/j.ocemod.2008.06.009)
- Woth K, Weisse R, Storch H (2005) Climate change and North Sea storm surge extremes: an ensemble study of storm surge extremes expected in a changed climate projected by four different regional climate models. *Ocean Dyn* 56:3–15. doi:[10.1007/s10236-005-0024-3](https://doi.org/10.1007/s10236-005-0024-3)